Electronic Supplementary information (ESI)

A facile synthesis for layered double hydroxide based core@shell hybrid materials

Meng Lyu, Chunping Chen, Jean-Charles Buffet, and Dermot O'Hare

Chemistry Research Laboratory, Department of Chemistry, University of Oxford, 12 Mansfield Road, Oxford, OX1 3TA, UK.

Table of Contents

1. Experimental details

1.1. General information

1.1.1. Materials

Zeolite 13X (Si/Al 1.23:1, Alfa Aesar); magnesium nitrate hexahydrate ($Mg(NO_3)_2 \cdot 6H_2O$, AR, Sigma-Aldrich); aluminum nitrate nonahydrate ($Al(NO_3)_3) \cdot 9H_2O$, AR, Sigma-Aldrich); sodium hydroxide (NaOH, AR, Sigma-Aldrich); sodium carbonate (Na_2CO_3, AR, Sigma-Aldrich); 2,5-Dihydroxyterephthalic acid (H_4DHTP, AR, Fluorochem). All chemicals and materials were used without further purification. All reference to 'water' or 'H_2O' refer to deionised water.

1.2. Synthesis of Mg-MOF-74

Mg-MOF-74 was synthesised according to the revised method reported in the literature. $Mg(NO_3)_2 \cdot 6H_2O$ (0.67 g, 2.60 mmol) was dissolved in a solvent mixture (70 mL) of *N,N*-dimethylformamide (DMF), ethanol and DI water (15: 1: 1, v/v/v) with 2,5-dihydroxybenzene carboxylic acid (0.16 g, 0.78 mmol) and trimethylamine (TEA, 0.1 mL) under stirring. The resulting mixture was placed in a 100 mL Duran bottle and heated at 125 °C for 24 hours under static condition to afford dark-yellow crystals. The solid was collected by filtration and washed with DMF (3 X 20 mL) and methanol before being soaked in methanol (70 mL). The methanol was decanted and replaced three times for three days. Finally, the solid was collected by filtration and dried under vacuum at 30 °C overnight

1.3. Characterisation

Powder X-ray diffraction (PXRD) analysis was carried out using a PANAnalytical X'Pert Pro Diffractometer in scanning mode using Cu Kα radiation ($\alpha1 = 1.540598$ Å, $\alpha2 = 1.544426$ Å). The sample was packed on a stainless steel holders which resulted in peaks at 43.36, 44.29, and 50.51° which did not interfere with the analysis. Signals between $2\theta = 3$ - 70° were recorded with step size 0.0167°. Pawley and Retvield refinement were conducted using TOPAS-Academic V6.[1]

Scanning electron microscopy (SEM) images and Energy dispersive X-ray spectroscopy (EDS) mappings were obtained from a JOEL JSM-6610LV low vacuum scanning electron microscope at the Harwell Research Complex with an accelerating voltage of 10 kV or a Zeiss EVO scanning electron microscope with an accelerating voltage of 5 kV.

Transmission electron microscopy (TEM) images, EDS mappings were obtained from a JEOL-2100 electron microscope at the Harwell Research Complex with an accelerating voltage of 200 kV using a single tilt specimen.

Fourier transform Infrared spectroscopy (FTIR) was conducted using a ThermoScientific Nicolet iS5 spectrometer fitted with an iD3 attenuated total reflection stage. Signals between 4000 – 700 cm^{-1} wavelength were recorded at 4 cm^{-1} resolution.

The solid-state DPMAS ^{27}Al and DPMAS ^{29}Si nuclear magnetic resonance (NMR) spectra were obtained on a Bruker Avance IIIHD spectrometer using 4.0 mm O.D zirconia rotors by Dr. Nick Rees, University of Oxford. The ^{27}Al NMR spectroscopy was recorded at 104.2 MHz (9.4 T) at a MAS rate of 10 kHz. A single pulse excitation was applied using a short pulse width (0.23 μs) to get the quantitative MAS spectra. Typically, 16725 scans were acquired with a 0.1 s delay. The ^{27}Al chemical shifts in the spectroscopy are referenced to the aqueous solution of $Al(NO_3)_3$ (0 ppm).

The ^{29}Si NMR spectroscopy was recorded at 79.4 MHz (9.4 T) at a 10 kHz spinning. An one-pulse sequence and spinal64 proton decoupling was applied to get the quantitative MAS spectra. Typically, 2619 transients were acquired with a 30 s delay. The ^{29}Si chemical shifts are referenced to kaolinite (with chemical shift $\delta = -91.7$ ppm on a scale where δ (TMS) = 0) as a secondary reference.

Thermogravimetric analyses (TGA) were performed under nitrogen atmosphere using PerkinElmer TGA 8000. The weight change between 30 – 800 °C was recorded with 5 °C/min ramp rate.

Elemental analyses (EA) were performed by Mr. Setphen Boyer at the Science Centre, London Metropolitan University. The quantitative oxidative combustion technique was applied to test the carbon, hydrogen nitrogen weight percent in the sample. Two measurements were taken and the average value was reported.

Inductively coupled plasma mass spectrometry (ICP-MS) analyses were performed by Dr. Alaa Abdul-Sada at University of Sussex using an Agilent 7500 series ICP-MS in helium collision mode to obtain the weight percent of sodium, magnesium, aluminium, silicon in the sample. Approximately 10 mg of sample was digested in concentrated nitric acid. The mixture was then diluted by a factor of 10 with dilute nitric acid before the analysis. Each mixture was analysed for three times and the average value was reported.

Brunauer-Emmett-Teller (BET) method analysis was carried out using a Micromeritics 3Flex. The N_2 adsorption and desorption of samples were taken at -196 °C. Before the measurement, Z13X, Z13X@Mg_2Al-CO_3 LDH and Mg_2Al-CO_3 LDH were *ex-situ* degassed overnight at 200 °C and then *in-situ* degassed at 200 °C for 3 hours. Before the measurement, Mg-MOF-74 and MOF@Mg_2Al-CO_3 LDH were *in-situ* degassed at 250 °C for 5 hours.

2. Additional Characterising Data

2.1. Z13X@Mg_2Al LDH

2.1.1. SEM data

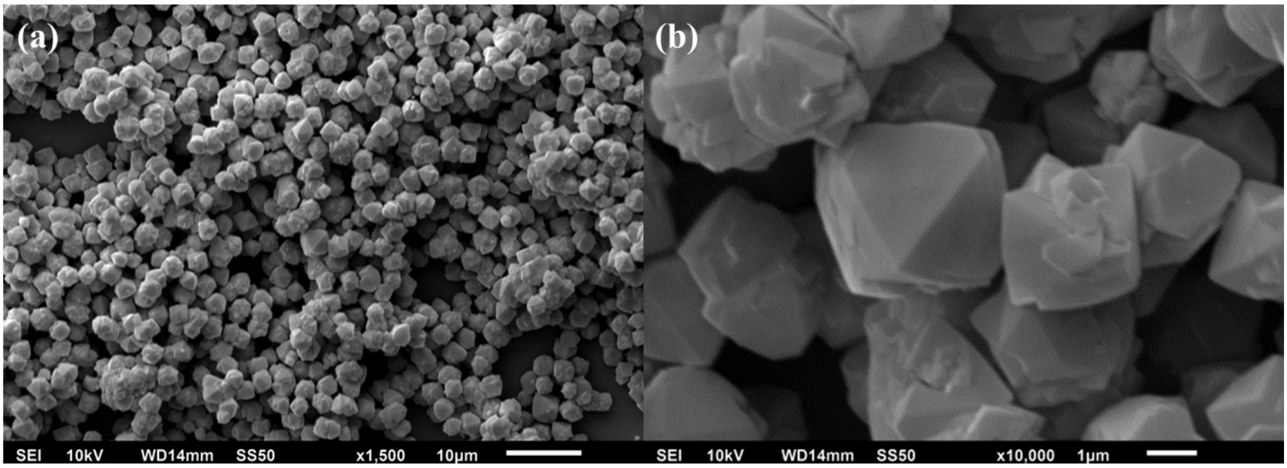

Fig. S1. The SEM image of the commercial Zeolite 13X (a) at the 10 μm scale and (b) at the 1 μm scale.

2.1.2. XRD data and Pawley refinement

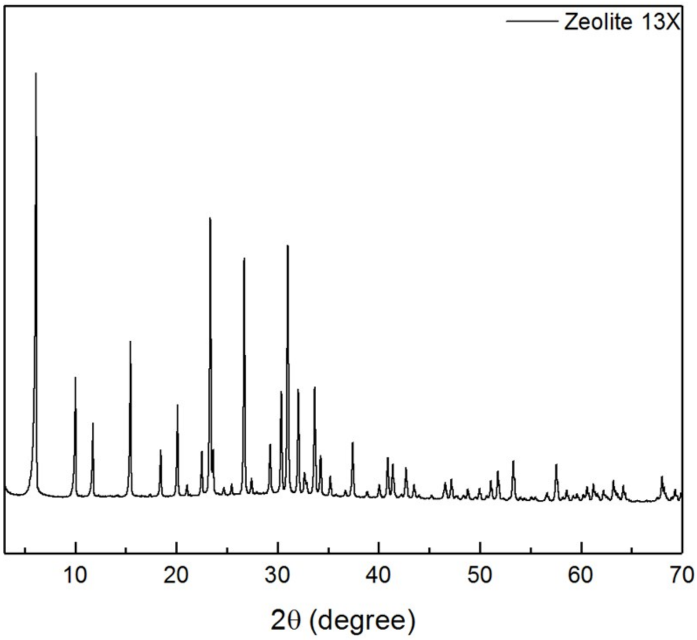

Fig. S2. The PXRD pattern of the original Zeolite 13X (Z13X).

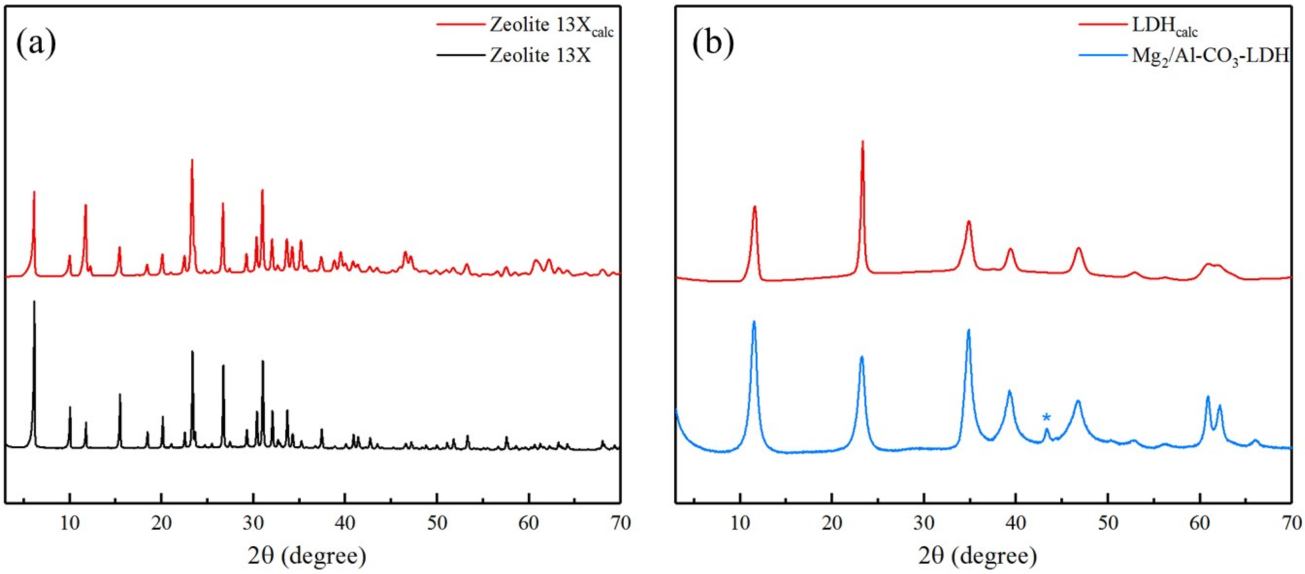

Fig. S3. XRD patterns of (a) the commercial Z13X (black) and the extracted individual phase of Z13X in Z13X@Mg_2Al-CO_3 LDH from the Pawley refinement (red) and (b) Mg_2Al-CO_3 LDH (blue) and the extracted individual phase of LDH in Z13X@Mg_2Al-CO_3 LDH from the Pawley refinement (red). * indicates peak rising from sample holder.

Table S1. Refinement details for **Z13X@Mg_2Al LDH** PXRD.

Single phase component	Zeolite 13X	LDH
Crystal system	Fajusite	Rhombohedral (Hexagonal setting)
Space group	Fd -3	R -3m :H
a / Å	24.970	3.046
b / Å	24.970	3.046
c / Å	24.970	22.96
α/ °	90	90
β/ °	90	90
γ/ °	90	120
λ/ Å	1.5406	
Refinement type	Pawley	
Rp / %	4.682	
Rwp / %	6.578	
Rp’ /%	8.989	
Rwp’ / %	10.720	
Software	TOPAS-Academic V6	

2.1.3. FTIR data

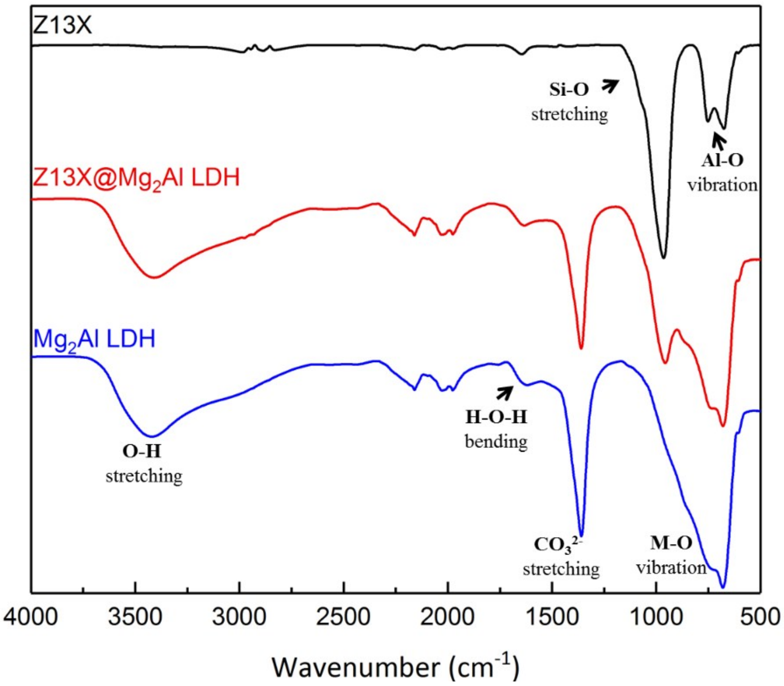

Fig. S4. The FTIR spectra of the Z13X (black), Z13X@Mg$_2$Al-CO$_3$ LDH (red) and Mg$_2$Al-CO$_3$ LDH (blue). Features around 2000 cm^{-1} are signals from sample stage.

2.1.4. Solid state NMR spectroscopy data

Table S2. Silicon environment in Z13X and Z13X@Mg$_2$Al LDH from ^{29}Si MAS solid-state NMR spectroscopy.

Assignment	**Z13X**		**Z13X@Mg$_2$Al LDH**	
	Position	Integration	Position	Integration
Q^{4}Si(4Al)	-84.2	41.96%	-84.4	34.43%
Q^{4}Si(3Al)	-88.8	27.38%	-89.1	23.68%
Q^{4}Si(2Al)	-93.5	15.82%	-94.0	13.33%
Q^{4}Si(1Al)	-98.1	4.51%	-98.8	4.51%
Q^{4}Si(0Al)	-102.0	3.88%	-103.4	9.86%
	-111.2	5.75%	-110.9	9.74%
	-117.7	0.69%	-116.9	4.44%

Equation S1. Loewenstein's rule equation.[2–4]

$$\frac{\mathrm{Si}}{\mathrm{Al}} = \frac{\sum_{x=0}^{4} I_{\mathrm{Si(OAl)}_x}}{0.25\sum_{x=0}^{4} x I_{\mathrm{Si(OAl)}_x}}$$

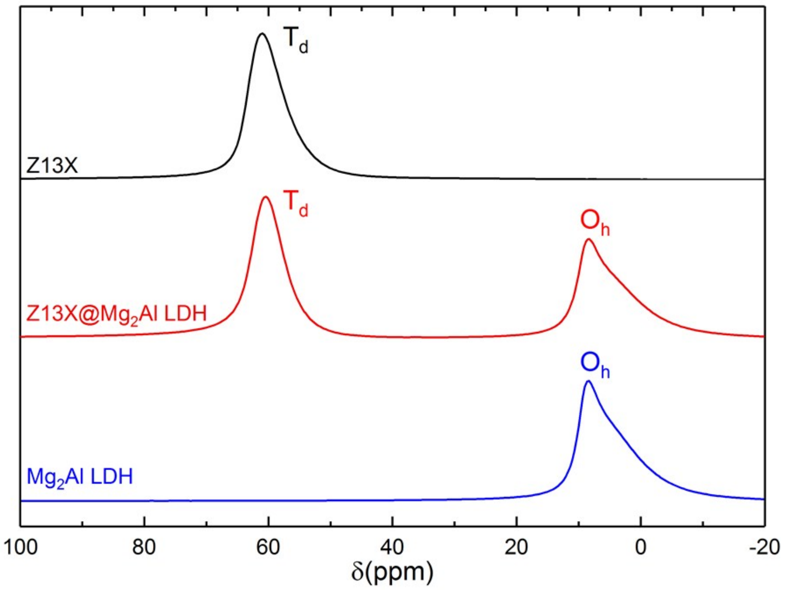

Fig. S5. ^{27}Al DP-MAS ssNMR spectra of the Z13X (black), Z13X@Mg_2Al-CO_3 LDH (red) and Mg_2Al-CO_3 LDH (blue). Two overlapped octahedral Al peaks can be observed from the Mg_2Al-CO_3 LDH and Z13X@Mg_2Al-CO_3 LDH ^{27}Al ssNMR spectra.[5]

2.1.5. TGA data

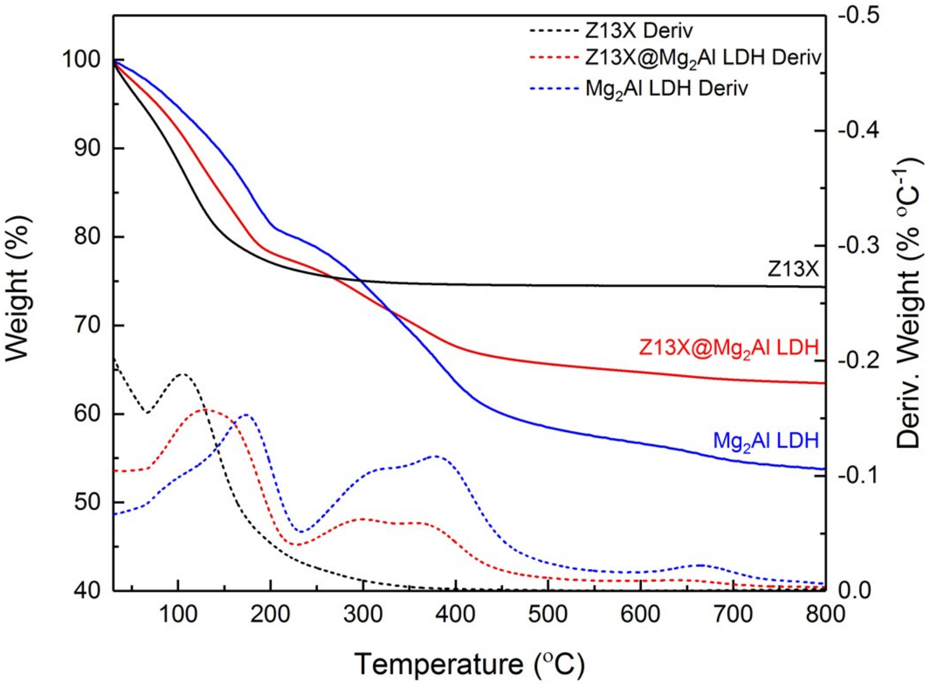

Fig. S6. TGA and DTG plots of the Z13X (black), Z13X@Mg_2Al-CO_3 LDH (red) and Mg_2Al-CO_3 LDH (blue).

2.1.6. N_2 adsorption-desorption isotherms and porosity data

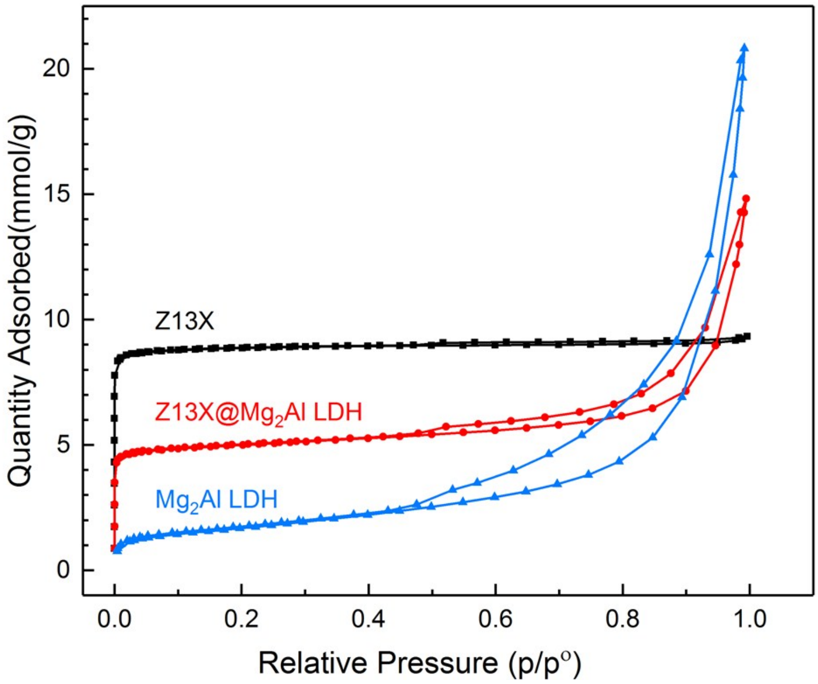

Fig. S7. N_2 adsorption-desorption isotherm of the Z13X (black), Z13X@Mg_2Al-CO_3 LDH (red) and Mg_2Al-CO_3 LDH (blue).

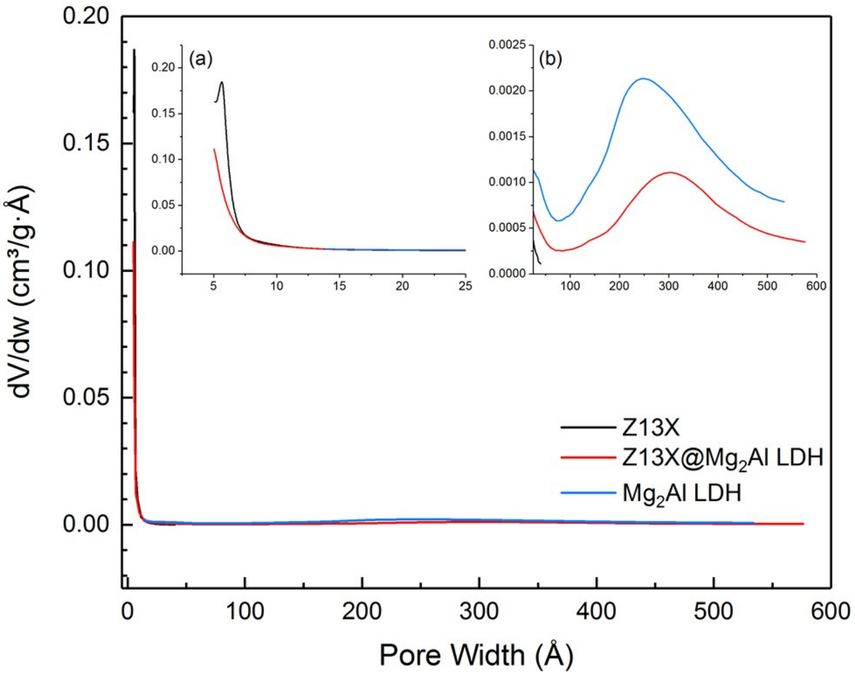

Fig. S8. Pore size distribution of the Z13X (black), Z13X@Mg_2Al-CO_3 LDH (red) and Mg_2Al-CO_3 LDH (blue). (a) is the zoom-in of 2.5-25 Å pore width and (b) is the zoom-in of 25-600 Å pore width.

2.2. Z13X@Mg_2Al LDHs with varied dropping time and ageing time

2.2.1. XRD data

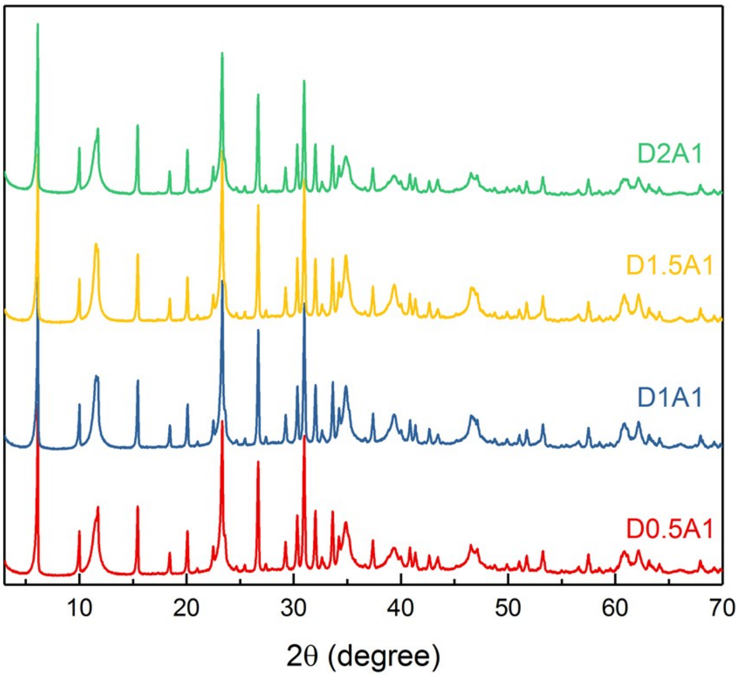

Fig. S9. XRD spectra of Z13X@Mg_2Al-CO_3 LDHs with different dropping time.

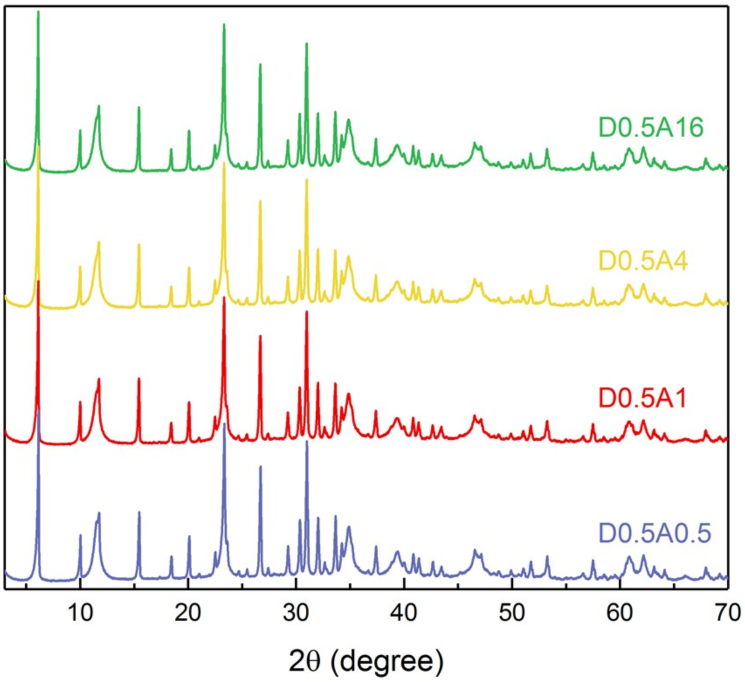

Fig. S10. XRD spectra of Z13X@Mg_2Al-CO_3 LDHs with different ageing time.

2.2.2. *TEM images*

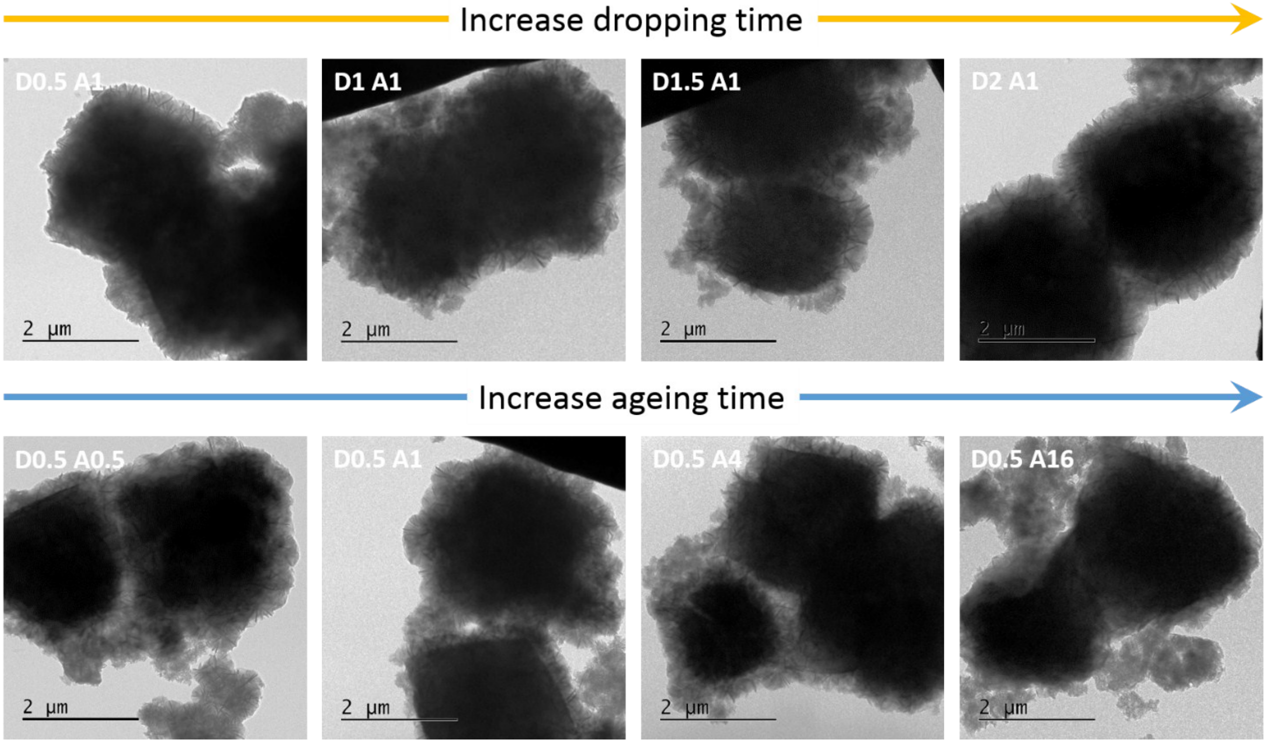

Fig. S11. TEM images of Z13X@Mg_2Al-CO_3 LDH core-shells with different dropping time and ageing time.

2.2.3. *TGA plots*

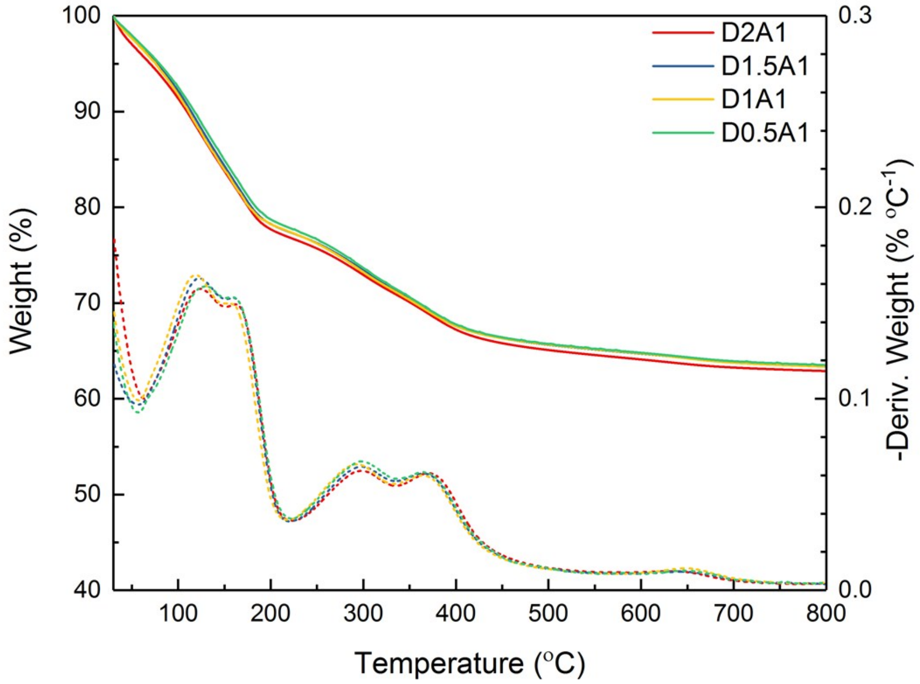

Fig. S12. TGA plots of Z13X@Mg_2Al-CO_3 LDH core-shells with different dropping time.

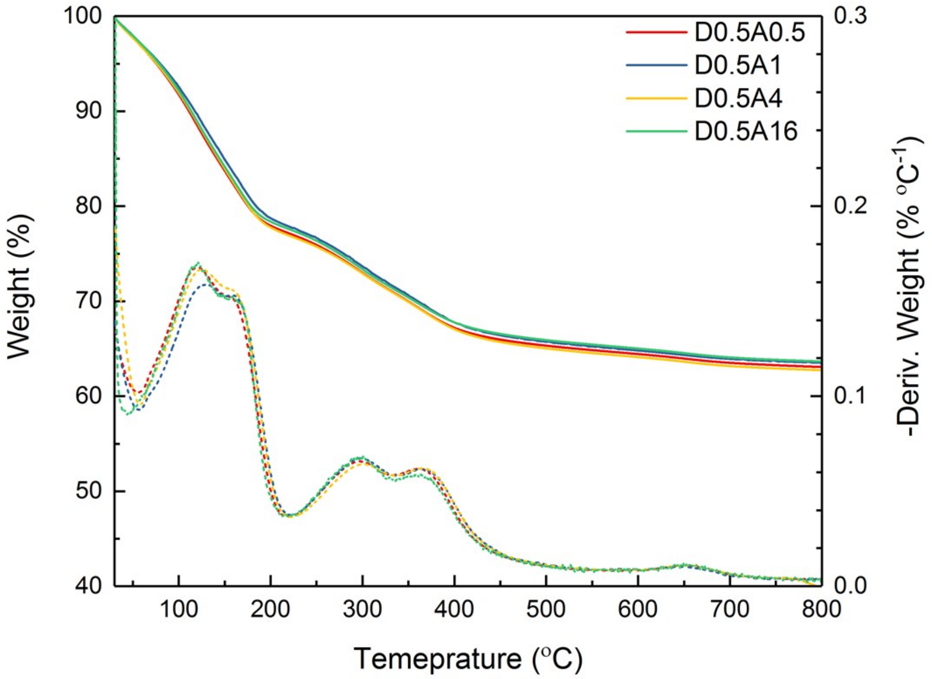

Fig. S13. TGA plots of Z13X@Mg_2Al-CO_3 LDH core-shells with different ageing time.

2.2.4. BET specific surface area data

Table S3. Summary of the N_2 BET specific surface areas and pore volumes of Z13X@Mg_2Al-CO_3 LDH with varied dropping time and ageing time

Entry	**Samples**	**Surface area (m^2/g)**			**Micropore Volume (cm^3/g)**
		BET	External	Micropore	
1	D2A1	449± 0.44	67	382	0.14626
2	D1.5A1	458± 0.67	72	386	0.14888
3	D1A1	505± 0.66	73	432	0.16626
4	D0.5A1	494± 0.74	81	413	0.15955
5	D0.5A0.5	517± 0.76	77	440	0.16951
6	D0.5A4	466± 0.55	69	397	0.15272
7	D0.5A16	513± 0.45	87	426	0.16713

2.3. Mg-MOF-74@Mg_2Al-CO_3 LDHs

2.3.1. XRD of Mg-MOF-74

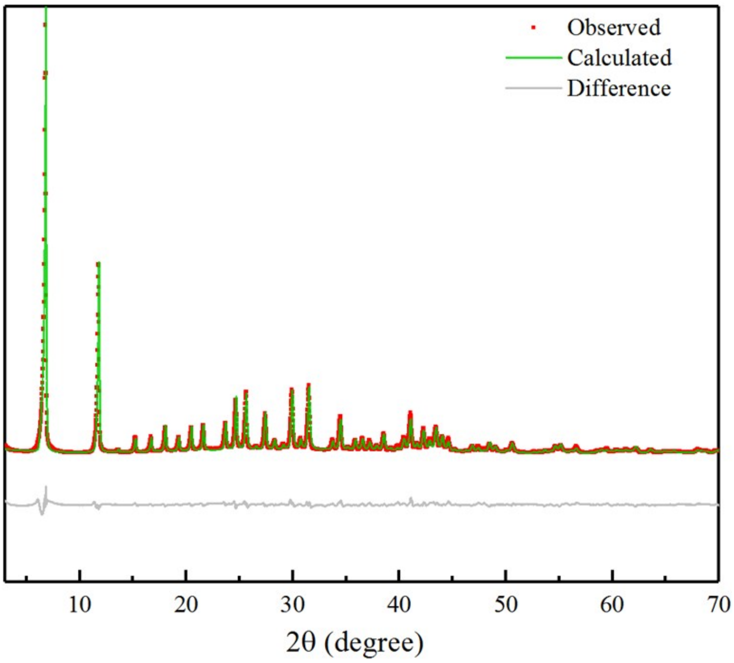

Fig. S14. Powder XRD pattern and the single-phase Rietveld refinement of Mg-MOF-74. Recorded experimental result is indicated in red; model built from TOPAS's calculation in green; difference between the real pattern and the refined model in grey. Mg-MOF-74 starting model is obtained from reference.[6]

Table S4. Refinement details for the Mg-MOF 74.

Atom	x	y	z	Occupancy
C(1)	0.40274	0.42351	0.73851	1.0
C(2)	0.46950	0.47795	0.85329	1.0
C(3)	0.49803	0.51164	0.75835	1.0
C(4)	0.55037	0.53720	0.99410	1.0
Mg(1)	0.65197	0.61578	0.63513	1.0
O(1)	0.40445	0.43862	0.57932	1.0
O(2)	0.36645	0.38301	0.78409	1.0
O(3)	0.57538	0.60473	0.83944	1.0
O(4)	0.66111	0.54389	0.79751	1.0
O(5)	0.68955	0.53470	0.18493	1.25
O(6)	0.74074	0.49972	0.63560	1.25
O(7)	0.70875	0.39779	1.08924	1.25
O(8)	0.56277	0.15467	0.49006	1.25
a = 26.018692 Å; c= 6.789166 Å; Volume = 3980.320 Å^3 Space group: *R-3*; R_{wp} = 7.34058638%				

2.3.2. Retvield refinement details of Mg-MOF-74@Mg_2Al-CO_3 LDH

Table S5. Two-phase refinement details for the Mg-MOF 74@Mg_2Al-CO_3 LDH.

Phase 1: Mg-MOF-74				
Atom	**x**	**y**	**z**	**Occupancy**
C(1)	0.40113	0.41958	0.7468	1.0
C(2)	0.45333	0.45781	0.8862	1.0
C(3)	0.49620	0.51598	0.7891	1.0
C(4)	0.54217	0.55212	0.9258	1.0
Mg(1)	0.65048	0.61512	0.64538	1.0
O(1)	0.40416	0.43959	0.5674	1.0
O(2)	0.36180	0.37120	0.8109	1.0
O(3)	0.58373	0.60612	0.8426	1.0
O(4)	0.65528	0.54450	0.7926	1.0
O(5)	0.69465	0.54725	0.1893	1.25
O(6)	0.7468	0.50561	0.6644	1.25
O(7)	0.7338	0.3535	1.0816	1.25
O(8)	0.5540	0.41958	0.5088	1.25
a = 26.003838 Å; c= 6.779764 Å; Volume = 3974.05 $Å^3$ Space group: *R-3*.				
Phase 2: Mg_2Al-CO_3 LDH				
Atom	**x**	**y**	**z**	**Occupancy**
Mg	0.00000	0.00000	0.00000	0.28465
Al	0.00000	0.00000	0.00000	0.67856
O(1)	0.00000	0.00000	0.38577	1.0
O(2)	0.125	-0.125	0.50000	1.0
C	0.33333	0.66667	0.50000	1.0
a = 3.04067 Å; c= 22.985763 Å; Volume = 184.843 $Å^3$ Space group: *R-3m:H*; R_{wp} = 7.34058638%				

2.3.3. FTIR data

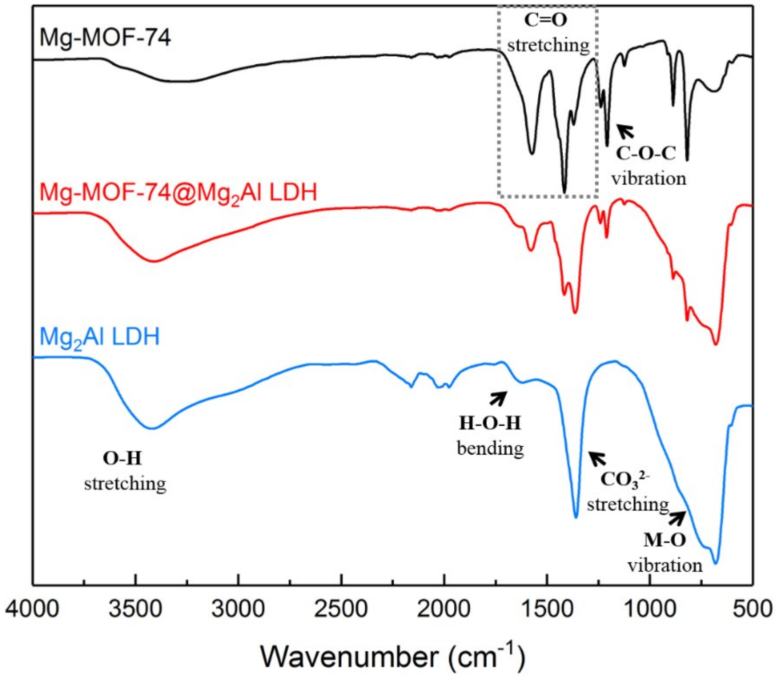

Fig. S15. The FTIR spectra of the Mg-MOF-74 (black), Mg-MOF-74@Mg_2Al-CO_3 LDH (red) and Mg_2Al-CO_3 LDH (blue). Features around 2000 cm^{-1} are signals from sample stage.

2.3.4. TGA data

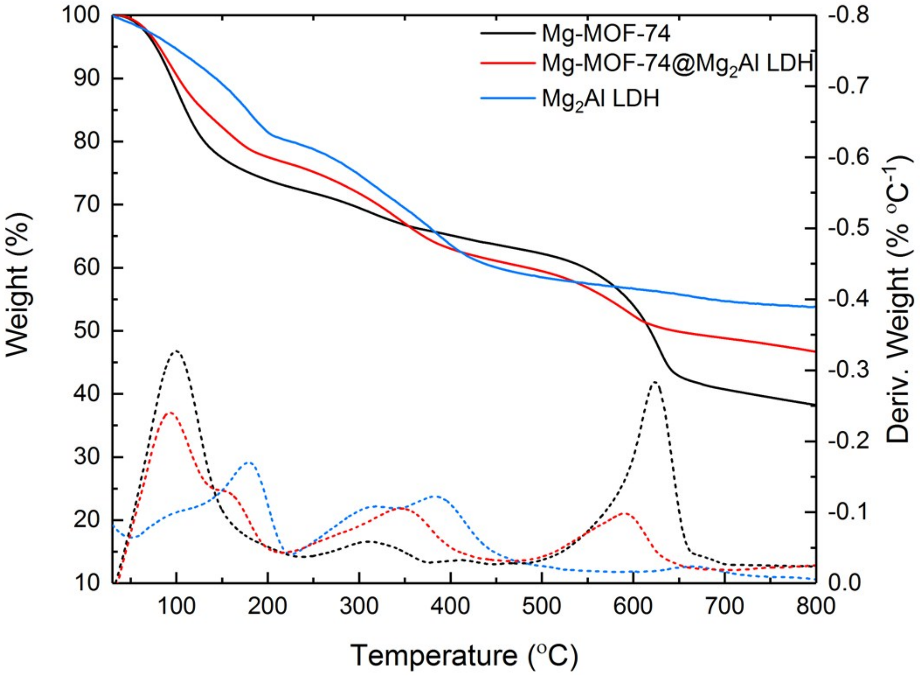

Fig. S16. The TGA plots of the Mg-MOF-74 (black), Mg-MOF-74@Mg_2Al-CO_3 LDH (red) and Mg_2Al-CO_3 LDH (blue).

2.3.5. N_2 adsorption-desorption isotherms and BET specific surface area

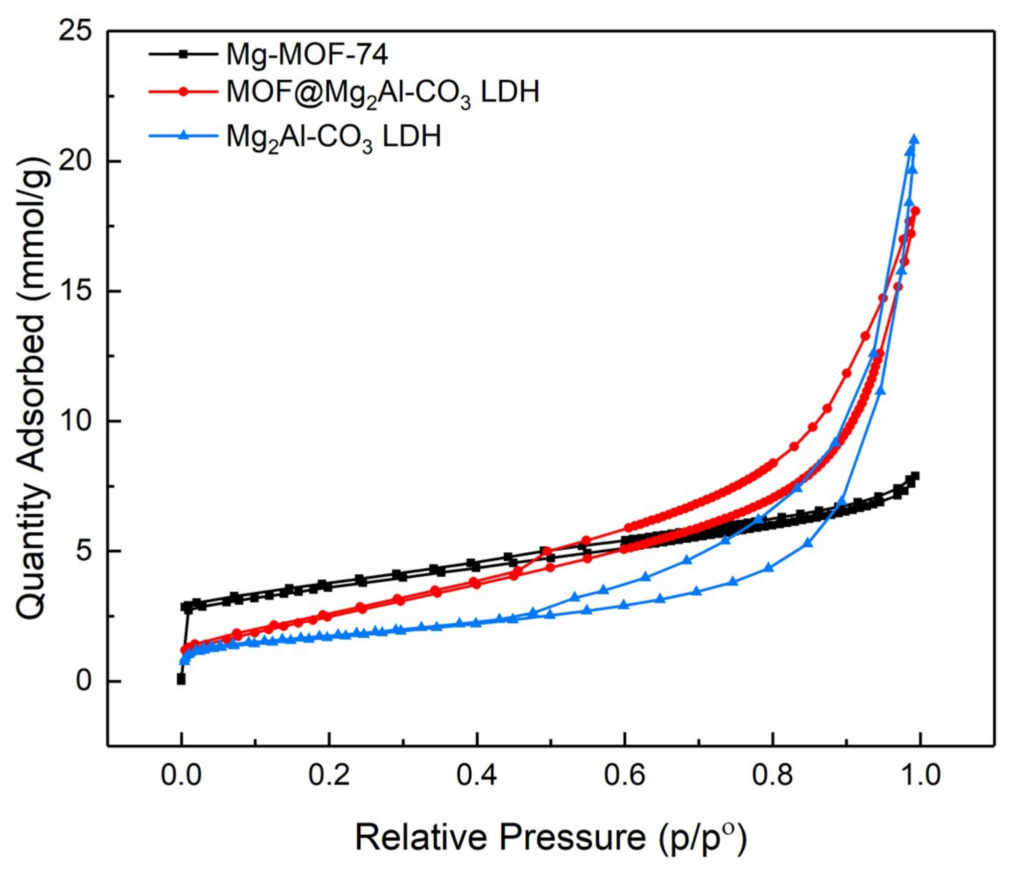

Fig. S17. N_2 adsorption-desorption isotherm of the Mg-MOF-74 (black), MOF@Mg_2Al-CO_3 LDH (red) and Mg_2Al-CO_3 LDH (blue).

Table S6. Summary of the N_2 BET specific surface areas and pore volumes of MOF@Mg_2Al-CO_3 LDH with varied dropping time and ageing time.

Samples	**Surface area (m^2/g)**			**Micropore Volume (cm^3/g)**
	BET	External	Micropore	
Mg-MOF-74	284 ± 0.52	81.34	202.65	0.036686
MOF@Mg_2Al-CO_3 LDH	234 ± 2.11	234	0	0
Mg_2Al-CO_3 LDH	134 ± 0.13	133.54	1.32	0.16626

3. Reference

1 A. A. Coelho, TOPAS-Academic (Version 6), Coelho Software, Brisbane, Australia, 2016.

2 F. Dogan, K. D. Hammond, G. A. Tompsett, H. Huo, W. C. Conner, S. M. Auerbach and C. P. Grey, *J. Am. Chem. Soc.*, 2009, **131**, 11062–11079.

3 W. Loewenstein and M. Lowenstein, *Am. Mineral.*, 1954, **39**, 92–96.

4 C. A. Fyfe, Y. Feng, H. Grondey, G. T. Kokotailo and H. Gies, *Chem. Rev.*, 1991, **91**, 1525–1543.

5 P. J. Sideris, U. G. Nielsen, Z. Gan and C. P. Grey, *Science*, 2008, **321**, 113–117.

6 P. D. C. Dietzel, R. Blom and H. Fjellvåg, *Eur. J. Inorg. Chem.*, 2008, **23**, 3624–3632.